Microscopic Modelling of Quantum Well Solar Cells

U. Aeberhard and R. Morf

Condensed Matter Theory, Paul Scherrer Institut, CH-5232 Villigen, Switzerland
{urs.aeberhard|rudolf.morf}@psi.ch

Abstract

We present a microscopic model of the photocurrent in quantum well solar cells (QWSC), based on the non-equilibrium Green's function formalism (NEGF) for a multiband tight-binding Hamiltonian. The quantum kinetic equations are self-consistently coupled to Poisson's equation. Relaxation and broadening mechanisms are considered by the inclusion of acoustic and optical electron-phonon interaction in a self-consistent Born approximation of the scattering self energies. Results are shown for the density of states, spectral response, current spectrum and IV-characteristics of single quantum well *pin*-structures.

1 Introduction

Since the pioneering work of Barnham and co-workers [1], the potential efficiency enhancement by the introduction of quantum wells in the intrinsic region of a *pin* solar cell has attracted considerable interest both from the photovoltaic community and within a broad spectrum of fundamental research [2].

A consistent description of the optical and transport processes in QWSC (Fig.1) requires the combination of a microscopic material model with a formalism for non-equilibrium quantum transport in interacting systems. The NEGF formalism together with a tight-binding or Wannier basis matches these requirements and has been successfully applied to similar systems like quantum cascade lasers [3], infrared photodetectors [4] or resonant tunneling in layered semiconductor heterostructures [5].

Generation and recombination

1. Photogeneration of electron-hole pairs
2. Radiative recombination
3. Nonradiative recombination

Transport

1. Resonant and nonresonant tunneling
2. Thermal escape and sweep-out
3. Relaxation by inelastic scattering
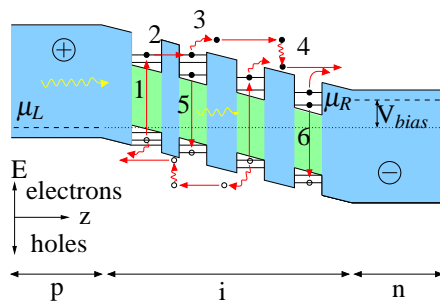
Figure 1: Characterizing structure and processes of a *pin*-QWSC.

2 Model

The QWSC system is described by the total Hamiltonian

$$H = H_0 + H_{int}, \quad H_{int} = H_{ep} + H_{e\gamma} + H_{other}, \tag{1}$$

where H_0 contains the kinetic energy, band structure effects and the Hartree potential, H_{ep} and $H_{e\gamma}$ stand for the interaction of carriers with phonons and photons, respectively, and H_{other} contains further types of elastic scattering (from interface roughness, ionized dopants, alloy composition inhomogeneities, etc.), inter-carrier scattering and nonradiative recombination terms, which will not be discussed in the present work. The Hamiltonians of the extended contact regions are absorbed into respective boundary self energies Σ^B reflecting the openness of the system. Interactions such as carrier-phonon and carrier-photon scattering are included perturbatively in terms of interaction self energies Σ on the level of a self-consistent Born approximation. For polar-optical phonons, which are the main relaxation mechanism, the standard Fröhlich Hamiltonian is used, and the acoustic phonons are modelled by the deformation potential approach. The coupling to photons is described within the dipole approximation and for monochromatic illumination. For both phonons and photons, an equilibrium distribution is assumed. Carrier-carrier interactions are considered by solving the macroscopic Poisson's equation for the electrostatic potential with the carrier densities from the Green's functions and a given doping profile, which corresponds to a Hartree level approximation.

The real time non-equilibrium Green's functions $G_{\alpha,L;\alpha',L'}(\mathbf{k};t,t')$, with L, α indicating layer and atomic orbital and $\mathbf{k}$ the transverse momentum, are defined as the non-equilibrium ensemble averages of the corresponding single-particle operators [6, 7]. In steady state, it is possible and more convenient to work with the Fourier transform $G^<_{\alpha,L;\alpha',L'}(\mathbf{k};E)$.

Within the NEGF formalism, the steady state equations of motion for the Green's function are given (in matrix notation) by the Dyson equations

$$G^R = \left[\left(G_0^R\right)^{-1} - \Sigma^R - \Sigma^{RB} \right]^{-1}, \quad G_0^R = \left[(E + i\eta)1 - H_0\right]^{-1}, \tag{2}$$

$$G^< = G^R \left(\Sigma^< + \Sigma^{<B}\right) G^A, \quad G^A = (G^R)^\dagger, \quad G^> = G^< + G^R - G^A. \tag{3}$$

Together with the self-energies from boundaries and interactions, they form a closed set of equations for the Green's functions that has to be solved self-consistently. For the solution of Eqs. 2 and 3, a recursive algorithm is used.

Once the Green's functions are known, macroscopic quantities can be derived, such as carrier and current densities at a given layer L, which for a nearest-layer coupling tight-binding model are given by

$$n(p)_L = \frac{\mp 2i}{A\Delta} \sum_{\mathbf{k}} \int \frac{dE}{2\pi} tr\{G^{<(>)}_{L;L}(\mathbf{k};E)\}, \tag{4}$$

$$J_L^{n(p)} = \frac{2e}{\hbar A} \sum_{\mathbf{k}} \int \frac{dE}{2\pi} tr\{t_{L;L+1} G^{<(>)}_{L+1;L}(\mathbf{k};E) - G^{<(>)}_{L;L+1}(\mathbf{k};E) t_{L+1;L}\}, \tag{5}$$

where A is the cross sectional area, and the trace is over orbital indices.

3   Results

The results shown in the following were obtained using a two band nearest-layer coupling tight bin~~ding model for a~~ $Al_xGa_{1-x}As$ type *pin*-diode with quantum wells of *GaAs* embedded in the intrinsic region. The tight-binding Hamiltonian yields the band structure in transport direction (z), whereas for the transverse band structure a parabolic and isotropic approximation is used. To reduce the computational burden, short structures with low band gaps, but comparable built-in fields were investigated.

3.1   Local density of states

The local density of states (LDOS) at layer L is given by

$$\rho_L(E) = \sum_{\mathbf{k}} tr\{A_{L;L}(\mathbf{k};E)\}, \quad A = i(G^R - G^A), \tag{6}$$

where A is the spectral function. Fig.2 (left) displays the LDOS for a 25 monolayer (ML) single-quantum well structure with 60 ML highly doped ($N_{d,a} = \pm 10^{18} cm^{-3}$) contacts and intrinsic spacers of 55 ML. The two gap energies are $E_{g,low} = 0.5\ eV$ and $E_{g,high} = 1\ eV$, respectively, with a valence band offset of $0.2\ eV$. The transverse momentum integration is restricted to the relevant range at a given Fermi level. There are two confinement levels both in the conduction an the valence band. The level broadening is determined by the quantum well depth and the effective mass. In the valence band, inelastic electron-phonon scattering leads tho the formation of satellite peaks. Above the wells, additional structures from quasi-bound states and transmission resonances appear.
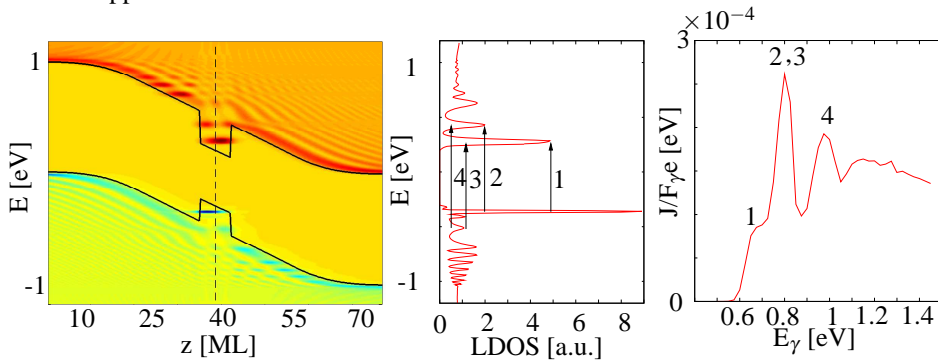
Figure 2: Local density of states (left), optical transitions (center) and spectral response for a 25 ML SQW device.

3.2   Optical transitions, photocurrent and spectral response

The relevant optical transitions and the corresponding spectral response or external quantum efficiency, defined as the short-circuit current normalized by the incoming photon flux, are shown in Fig.2 center and right, respectively. The contribution of lower-level transitions is suppressed due to the reduced escape rate (high barriers for

tunneling/thermoionic emission). The dominant contribution is due to the transitions between lower and higher levels, whereas contributions from higher transitions are reduced in magnitude due to lower occupation.

3.3   Current spectrum and IV-characteristics

The following results were obtained for the same structure with $E_{g,high} = 0.85\ eV$ and a valence band offset of $0.15\ eV$.

The current spectrum displayed in Fig.3 (left) shows the energy resolved contributions from photocurrent (positive) and dark current (negative for forward bias) to the total current. The photocurrent spectrum reflects the joint density of states of the dominant transition. The dark current spectrum shows the effects of relaxation by inelastic phonon scattering in terms of broadening towards lower energies.

Electron and hole currents grow within the illuminated region towards the respective contacts. The overall current is conserved, which is verified in Fig.3 (center).

The total current at the left interface to the interacting region is displayed in Fig.3 (right) as a function of the applied (forward) bias.
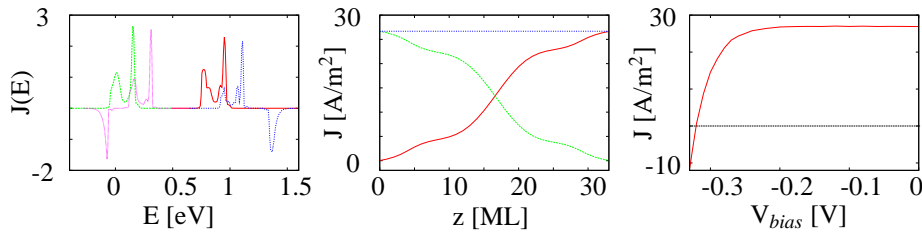
Figure 3: Current spectrum (left), current conservation (center) and IV-characteristics.

4   Conclusions

The non-equilibrium Green's function formalism applied to QWSC allows for a comprehensive study of the microscopic processes involved in the generation and transport of carriers under non-equilibrium conditions.

References

[1] K. Barnham and G. Duggan, J. Appl. Phys. **67**, 3490 (1990).

[2] K. Barnham et al., Physica E **14**, 27 (2002).

[3] S.-C. Lee and A. Wacker, Physica E **13**, 858 861 (2002).

[4] L. E. Henrickson, J. Appl. Phys **91**, 6273 (2002).

[5] R. Lake, G. Klimeck, R. C. Bowen, and D. Jovanovic, J. Appl. Phys **81**, 7845 (1997).

[6] L. P. Kadanoff and G. Baym, *Quantum Statistical Mechanics*, Benjamin-Cummings, 1995.

[7] L. Keldysh, Sov. Phys.-JETP. **20**, 1018 (1965).